



Detection of p62/SQSTM1 Aggregates in Cellular Models of CCM Disease by Immunofluorescence

Saverio Marchi, Saverio Francesco Retta, and Paolo Pinton

Abstract

Cerebral cavernous malformations (CCM) is a familial or sporadic rare disorder that is characterized by capillary vascular lesions with a mulberry-like appearance on MRI scans. Three distinct genes have been associated to CCM disease, known as *CCM1/KRIT1*, *CCM2/MGC4607*, and *CCM3/PDCD10*. Loss-of-functions mutations on these genes lead to deregulation in multiple signaling pathways, thereby resulting in disturbed vessel organization and function. Insufficient autophagy has been observed upon downregulation of all three *CCM* genes, both in cells and human patient tissues, revealed as aberrant accumulation of the autophagy receptor p62/SQSTM1. The autophagic process is conceived as an adaptive response to stress and is essential for the maintenance of cellular homeostasis. The aim of this review is to briefly summarize the current knowledge on the role of autophagy in CCM disease and to furnish a detailed protocol for detecting and measuring p62/SQSTM1 cytoplasmic aggregates through immunofluorescence technique.

Key words Cerebral cavernous malformations, p62/SQSTM1, Autophagy, mTORC1 signaling, Protein aggregates

1 Introduction

Cerebral cavernous malformations (CCMs) are common vascular malformations that occur frequently in the central nervous system. CCM lesions have a prevalence of about 0.1–0.5% in the general population [1, 2]. Usually, the symptomatology includes weakness, numbness, vision changes, or severe headache. Occasionally, seizures also can occur, as well as CCMs rupture, leading to hemorrhagic stroke or death. Although CCMs mostly occur as a single formation, about 20% of affected people have a familial (inherited) form of the disease. Indeed, CCMs have been linked to loss-of-function mutations in three distinct genes, named *CCM1* (*KRIT1*), *CCM2* (*MGC4607*), and *CCM3* (*PDCD10*) [3, 4]. The last 10 years of research on the molecular mechanisms underlie CCM disorder unequivocally revealed the pleiotropy of CCM genes since their inactivation leads to deregulation of

different cellular processes, including angiogenesis, redox homeostasis, endothelial-to-mesenchymal transition, and autophagy [5, 6].

1.1 The Autophagic Process: The Role of p62/SQSTM1

Macroautophagy (herein referred to as autophagy) and the ubiquitin-proteasome system (UPS) are the two major quality control pathways responsible for cellular homeostasis [7, 8]. Although UPS is deputized for the degradation of the majority of proteins, large intracellular structures, including damaged organelles (i.e., mitochondria), intracellular bacteria, or protein aggregates, are exclusively degraded by the autophagic route [9, 10]. At first, the selected cargos are sequestered into double-membrane vesicles, called autophagosomes, and after autophagosomes-lysosomes fusion, their degradation is mediated by lysosomal enzymes [11]. This occurs through the activity of specific elements, which are able to recognize selected substrates and designate them to autophagic degradation [12]. The class of proteins known as autophagic receptors include the p62/SQSTM1 (sequestosome-1) [13], NBR1 (neighbor of BRCA1) [14], NDP52 (nuclear dot protein 52 kDa) [15], Tax1BP [16], and Optineurin [17]. They share the capacity to identify degradation signals on cargo substrates and also interact with ATG8s, a family of proteins located in the inner surface of the forming autophagosome. In mammals, the prevailing autophagy-targeting label is ubiquitin, a small (8.6 kDa) signaling molecule that is bound to lysine residues by a sequential cascade that involves ubiquitin-activating (E1s) and -conjugating (E2s) enzymes, as well as ubiquitin ligases (E3s) [18].

The role of p62/SQSTM1 as an autophagy receptor mainly depends on three essential features: (1) p62/SQSTM1 employs its C-terminal UBA domain to bind to poly-ubiquitinated targets, although in some cases, the interaction occurs in an ubiquitin-independent manner; (2) it interacts with ATG8s through its LC3-interacting region (LIR); (3) p62/SQSTM1 polymerizes and co-aggregates with the target substrates, facilitating the conjugation of the complex with ATG8s in the forming autophagosome. This implies that p62/SQSTM1 aggregates are degraded together with the cargos by autophagy. In multiple autophagy-deficient contexts, as well as in various neurodegenerative diseases or liver diseases, p62/SQSTM1 accumulates in cytoplasmic and nuclear ubiquitinated inclusions [19–21]. Moreover, p62/SQSTM1 levels increase upon multiple stress signals, including oxidative stress, through a molecular route that involves the transcription factor NRF2 [22], or inflammation, via the NF- κ B pathway [23]. Under resting conditions, the amounts of autophagy receptors are kept low by continuous degradation. Conversely, during different stressful scenarios, p62/SQSTM1 production is rapidly boosted, reasonably to prevent the toxic accumulation of damaged/ubiquitinated structures. However, if there is no compensation by an adequate

autophagic response, such as in some chronic disorders, aberrant p62/SQSTM1 aggregates are formed inside the cytoplasm, thus representing a distinct pathological signature that could contribute to the progression of the disease.

1.2 Role of Autophagy in CCM

Our group recently showed a defect in the normal autophagic flux in cells depleted for *CCM1*, *CCM2*, or *CCM3* genes. We observed accumulation of p62/SQSTM1 clusters in CCM cells, leading to the formation of large intracellular aggregates, especially in the perinuclear area [24]. The insufficient autophagy is ascribed to higher activation of the mTORC1 (mechanistic Target of Rapamycin Complex 1) kinase, a master regulator of the autophagic process. Under nutrient-rich conditions, mTORC1 phosphorylates the ULK1/2 complex, thus inhibiting autophagy at early events by limiting the formation of autophagosomes [25]. Moreover, mTORC1 could affect autophagy by acting at the later stages of the process, through inhibition of lysosomal functions. Pharmacological inhibition of mTOR, using Rapamycin analogues, restores normal autophagic levels and mitigates other molecular derangements associated to CCMs, such as ROS (reactive oxygen species) overproduction and endothelial-to-mesenchymal transition [24]. The crucial role of mTOR-dependent autophagy inhibition in the pathogenesis of CCM is supported by other correlative observations, including vessel abnormalities in autophagy-deficient endothelial cells [26], the low autophagy levels in *CCM3*-depleted senescent cells [27], or overactive endothelial mTORC1 signaling in human arteriovenous malformations [28]. mTOR inhibitors are extensively used for the treatment of vascular anomalies [29], and different therapeutic approaches that have been proposed for CCM, such as Vitamin D3, statins, or sulindac sulfate, also trigger autophagy through mTOR inhibition [30]. Importantly, a recent pharmacological screening aimed to uncover novel molecules for the treatment of familial forms of CCM identified ridaforolimus as one of the few compounds able to induce some degree of rescue in multiple CCM models [31]. The non-prodrug, rapamycin analogue ridaforolimus acts as a potent mTOR inhibitor, showing a strong *in vivo* stability and antitumor activity [32].

Overall, there are several lines of evidence that deregulation of the mTOR signaling, with consequent suppression of the autophagic process, is one of the key events that arises from *CCM* genes loss-of-function, therefore contributing to CCM pathogenesis.

Here, we describe an immunofluorescence-based technique aimed to visualize and quantify p62/SQSTM1 aggregates in endothelial cell models of CCM. This method could be used to evaluate autophagy impairment in different pathological scenarios (not only CCM) or upon stimuli of various nature.

2 Materials

2.1 Cell Culture and Transfections

1. Human umbilical vein endothelial cells (HUVEC).
2. Medium 200.
3. Low serum growth supplement (LSGS).
4. 6-well and 24-well plates.
5. Lipofectamine™ RNAiMAX Transfection Reagent (Thermo Fisher Scientific, Cat. no. 13778150).
6. siRNA *CCM1* (Thermo Fisher Scientific, Cat. no. AM51331, ID 15469).
7. siRNA *CCM2* (Thermo Fisher Scientific, Cat. no. AM16708, ID 147904-05-06).
8. siRNA *CCM3* (Thermo Fisher Scientific, Cat. no. AM16708, ID 136322-23-24).
9. Silencer™ Negative Control No. 1 siRNA (Thermo Fisher Scientific, Cat. no. AM4611).

2.2 Immuno-fluorescence

1. Glass coverslips (13 mm).
2. Parafilm M.
3. 1× Phosphate buffered saline (PBS).
4. 4% Paraformaldehyde (PFA) solution. For 500 mL of 4% PFA, add 400 mL of 1× PBS to a glass beaker on a stir plate in a ventilated hood. Heat while stirring to approximately 50–55 °C. Pay attention that the solution does not boil. Add 20 g of PFA powder to the heated PBS and dissolve it overnight. Do not add NaOH. Adjust the volume to 500 mL with 1× PBS. The solution can be aliquoted and frozen at –20 °C.
5. Triton X-100 solution.
6. PBST or permeabilization solution: PBS + 0.05% Triton X-100.
7. Blocker Non-Fat Dry Milk.
8. PBSTM or blocking solution: PBST +5% Non-Fat Dry Milk.
9. Anti-p62/SQSTM1 antibody produced in rabbit (Sigma-Aldrich, Cat. no. P0067).
10. Goat anti-Rabbit IgG (H + L) Secondary Antibody, DyLight 594 (Thermo Fisher Scientific, Cat. no. 35560).
11. Microscope slides.
12. ProLong™ Diamond Antifade Mountant (Thermo Fisher Scientific, Cat. no. P36965).

2.3 Equipment Setup

p62 accumulation/aggregation could be imaged and recorded by using a confocal microscope, equipped with the appropriate filter set. Typically, correct sampling can be achieved by using 60× lens or higher with numerical aperture (N.A.) >1.3, and high-resolution CCD or CMOS cameras (with pixel size <8 μm). In this protocol, digital images were acquired with confocal microscope (Zeiss LSM510) using a 63 × 1.4 NA Plan-Apochromat oil-immersion objective.

3 Methods

3.1 Cell Culture and Transfections

1. Day 1: perform the *CCM1*, *CCM2*, or *CCM3* silencing in HUVEC cells using a “Reverse Transfection” protocol. Prepare complexes (siRNA(s) + RNAiMAX Transfection Reagent) inside the well, and then add cells and medium. Use a 6-well plate, with a final siRNA concentration of 40 nM in a final volume of 1 mL. In the “Reverse Transfection” protocol, a higher amount of cells (250–300.000 cells × well) is required. For *CCM2* and *CCM3* silencing, use a mix of the siRNAs indicated above (*see Note 1*).
2. Day 2: after 24 h, add 1 mL of medium in each well to reach a final volume of 2 mL (*see Note 2*).
3. Day 3: trypsinize cells and seed them on glass coverslips (13 mm in diameter), at a concentration of 50–60.000 cells per well.
4. Day 4: after 72 h of silencing, a % of knock-down >75 has been achieved (*see Note 3*).

3.2 Fixation, Permeabilization, and Blocking

1. Discard the medium and rinse quickly with PBS.
2. Place the 24-well plate on the top of ice and add 500 μL of cold 4% PFA solution for each well. Incubate for 10 min at 4 °C (*see Note 4*).
3. Wash three times with PBS for 10 min each under gentle shaking at room temperature (RT).
4. During incubation with PBS, prepare the PBST solution (*see Note 5*).
5. Add 500 μL of PBST and incubate for 10 min at RT.
6. Prepare the PBSTM solution (*see Note 6*).
7. Wash two times with PBS.
8. Add 1 mL of PBSTM. Incubate for 1 h at RT.

3.3 Antibodies Incubation

1. For the primary antibody incubation, firstly prepare a wet chamber. Use a Petri dish (150 mm in diameter) and cover it completely with tinfoil. On the bottom of the Petri, apply a layer of parafilm and fix it to avoid wrinkles or irregularities.

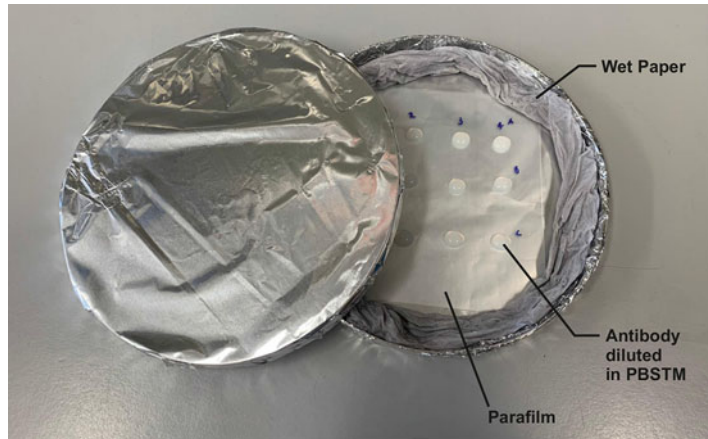


Fig. 1 Image of a wet chamber for immunofluorescence. The primary antibody is diluted in PBS + 0.05% Triton X-100 + 5% non-fat dry milk (PBSTM)

2. Dilute the p62/SQSTM1 primary antibody in PBSTM [dilution 1:50–1:75] (*see Note 7*).
3. For each sample, put 30 μ L of diluted antibody on the top of the parafilm (Fig. 1), paying attention to avoid bubbles formation.
4. Carefully remove the coverslips from the 24-well plate, gently drain them on clean paper and put on the wet chamber, ensuring that the cells are in direct contact with the antibody.
5. Add a piece of wet paper inside the chamber (Fig. 1) and incubate overnight at 4 °C.
6. Carefully place the coverslips in a new 24-well plate, and wash three times with PBS for 10 min each under gentle shaking at RT.
7. Dilute the Goat anti-Rabbit IgG (H + L) Secondary Antibody, DyLight 594 in PBSTM [dilution 1:500–1:1000] and protect it from light (*see Note 8*).
8. Add 1 mL of diluted secondary antibody per well and gently shake for 1 h at RT, protected from light.
9. Wash three times with PBS for 10 min each, under gentle shaking at RT, protected from light.
10. For each sample, put a drop of ProLong™ Diamond Antifade Mountant on a microscope slides.
11. Carefully remove the coverslips from the 24-well plate, gently drain them on clean paper and put on the microscope slide, ensuring that the cells are in direct contact with the Prolong.
12. Allow to dry for 2–3 h at RT (or overnight at 4 °C), protected from light (*see Note 9*).

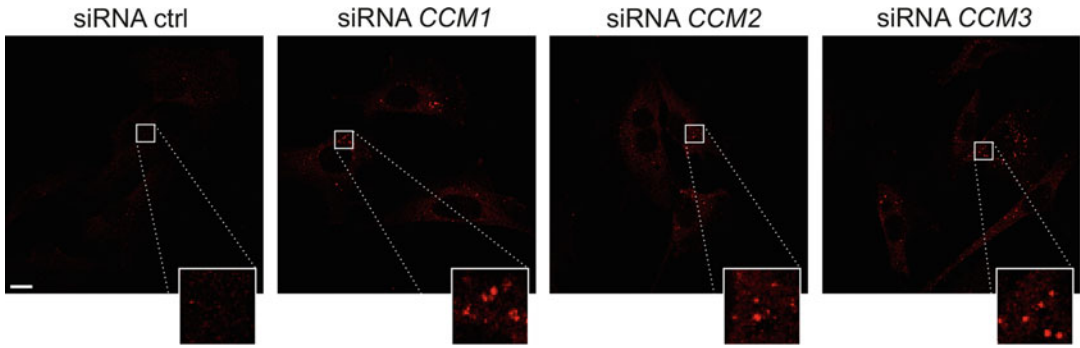


Fig. 2 Immunofluorescence images of HUVEC, silenced with the indicated siRNAs and stained for p62/SQSTM1. Note the numerous p62/SQSTM1 aggregates in *CCM1*-, *CCM2*-, and *CCM3*-silenced cells. Magnification in insets. Scale bar, 10 μm . Images were acquired with confocal microscope Zeiss LSM510

3.4 Microscope Acquisition of Images and Analysis

1. Add the immersion oil on the objective.
2. Place the slide on the microscope stage.
3. For high-resolution imaging, use the standard binning mode 1×1 (each logical pixel is equal to one physical pixel).
4. Acquire multiple images in manual mode or by using motorized stage, if the microscope is equipped. Use the same camera and microscope settings among the different conditions (*see Note 10*) (Fig. 2).
5. Open Fiji software [33] and load the files output.
6. Remove the background, setting the rolling ball to a size of approximately 1 μm (Menu Process \rightarrow Subtract Background).
7. Threshold image to isolate p62/SQSTM1 dots from background (Menu Image \rightarrow Adjust \rightarrow Threshold). Choose the most appropriate thresholding algorithms.
8. Measure/count p62/SQSTM1 dots using the “Analyze particles” tool (Menu Analyze \rightarrow Analyze particles). Set a minimum filter size to 2, check the “Pixel units” and “Display results” options (*see Note 11*).

4 Notes

1. HUVEC should be used at low passages number (2–6) to increase transfection efficacy.
2. If transfection induces massive cell death, discard the medium, wash two times with PBS, and add 2 mL fresh medium per well. Alternatively, increase the number of cells (up to 600–700.000 cells per well).
3. For *CCM1* silencing, transfection with a single siRNA (ID 15469) is sufficient to induce depletion of more than 90%.

4. To obtain a good p62/SQSTM1 staining, the 4% PFA solution has to be cool. If the solution was previously frozen, put it at 4 °C for 5–6 h (or the day before), allowing a slow defrost.
5. The amount of Triton X-100 can be increased up to 0.1%.
6. 5% Bovine serum albumin (BSA) can be used instead of non-fat dry milk.
7. It is important to prepare a negative control (without primary antibody) to recognize the non-specific signals that might derive from fluorescent dyes.
8. Other fluorescent-conjugated secondary antibodies (depending on the microscope filter set) can be used. We obtained good results with Goat anti-Rabbit IgG (H + L) Secondary Antibody, DyLight 488 (Cat. no. 35552).
9. To keep the coverslips in place, it could be useful to paint around the edges with nail varnish.
10. In order to obtain statistical significance, collect a number of at least 20 images per sample. Each condition should be prepared in triplicate and at least three independent experiments should be performed.
11. If the image contains multiple cells, divide the p62/SQSTM1 aggregates for the number of cells.

Acknowledgments

PP is grateful to Camilla degli Scrovegni for continuous support. This work was supported by the Italian Ministry of Health (GR-2016-02364602) and local funds from Marche Polytechnic University to SM; Telethon (GGP15219/B), the Italian Association for Cancer Research (AIRC: IG-23670), Progetti di Rilevante Interesse Nazionale (PRIN, 2017 E5L5P3) and local funds from the University of Ferrara to PP; Telethon (GGP15219/A) and local funds from the University of Torino to SFR.

References

1. Ene C, Kaul A, Kim L (2017) Natural history of cerebral cavernous malformations. *Handb Clin Neurol* 143:227–232. <https://doi.org/10.1016/B978-0-444-63640-9.00021-7>
2. Whitehead KJ, Smith MC, Li DY (2013) Arteriovenous malformations and other vascular malformation syndromes. *Cold Spring Harb Perspect Med* 3(2):a006635. <https://doi.org/10.1101/cshperspect.a006635>
3. Fischer A, Zalvide J, Faurobert E, Albiges-Rizo C, Tournier-Lasserre E (2013) Cerebral cavernous malformations: from CCM genes to endothelial cell homeostasis. *Trends Mol Med* 19(5):302–308. <https://doi.org/10.1016/j.molmed.2013.02.004>
4. Choquet H, Pawlikowska L, Lawton MT, Kim H (2015) Genetics of cerebral cavernous malformations: current status and future prospects. *J Neurosurg Sci* 59(3):211–220
5. Retta SF, Glading AJ (2016) Oxidative stress and inflammation in cerebral cavernous malformation disease pathogenesis: two sides of the

- same coin. *Int J Biochem Cell Biol* 81 (Pt B):254–270. <https://doi.org/10.1016/j.biocel.2016.09.011>
6. Lampugnani MG, Malinverno M, Dejana E, Rudini N (2017) Endothelial cell disease: emerging knowledge from cerebral cavernous malformations. *Curr Opin Hematol* 24 (3):256–264. <https://doi.org/10.1097/MOH.0000000000000338>
 7. Zientara-Rytter K, Subramani S (2019) The roles of ubiquitin-binding protein shuttles in the degradative fate of ubiquitinated proteins in the ubiquitin-proteasome system and autophagy. *Cell* 8(1). <https://doi.org/10.3390/cells8010040>
 8. Dikic I (2017) Proteasomal and autophagic degradation systems. *Annu Rev Biochem* 86:193–224. <https://doi.org/10.1146/annurev-biochem-061516-044908>
 9. Danieli A, Martens S (2018) p62-mediated phase separation at the intersection of the ubiquitin-proteasome system and autophagy. *J Cell Sci* 131(19). <https://doi.org/10.1242/jcs.214304>
 10. Janssen AFJ, Katrukha EA, van Straaten W, Verlhac P, Reggiori F, Kapitein LC (2018) Probing aggregatephagy using chemically-induced protein aggregates. *Nat Commun* 9(1):4245. <https://doi.org/10.1038/s41467-018-06674-4>
 11. Lamb CA, Yoshimori T, Tooze SA (2013) The autophagosome: origins unknown, biogenesis complex. *Nat Rev Mol Cell Biol* 14 (12):759–774. <https://doi.org/10.1038/nrm3696>
 12. Lamark T, Svenning S, Johansen T (2017) Regulation of selective autophagy: the p62/SQSTM1 paradigm. *Essays Biochem* 61 (6):609–624. <https://doi.org/10.1042/EBC20170035>
 13. Bjorkoy G, Lamark T, Brech A, Outzen H, Perander M, Overvatn A, Stenmark H, Johansen T (2005) p62/SQSTM1 forms protein aggregates degraded by autophagy and has a protective effect on huntingtin-induced cell death. *J Cell Biol* 171(4):603–614. <https://doi.org/10.1083/jcb.200507002>
 14. Kirkin V, Lamark T, Sou YS, Bjorkoy G, Nunn JL, Bruun JA, Shvets E, McEwan DG, Clausen TH, Wild P, Bilusic I, Theurillat JP, Overvatn A, Ishii T, Elazar Z, Komatsu M, Dikic I, Johansen T (2009) A role for NBR1 in autophagosomal degradation of ubiquitinated substrates. *Mol Cell* 33(4):505–516. <https://doi.org/10.1016/j.molcel.2009.01.020>
 15. Thurston TL, Ryzhakov G, Bloor S, von Muhlinen N, Randow F (2009) The TBK1 adaptor and autophagy receptor NDP52 restricts the proliferation of ubiquitin-coated bacteria. *Nat Immunol* 10(11):1215–1221. <https://doi.org/10.1038/ni.1800>
 16. Newman AC, Scholefield CL, Kemp AJ, Newman M, McIver EG, Kamal A, Wilkinson S (2012) TBK1 kinase addiction in lung cancer cells is mediated via autophagy of Tax1bp1/Ndp52 and non-canonical NF-kappaB signaling. *PLoS One* 7(11):e50672. <https://doi.org/10.1371/journal.pone.0050672>
 17. Wild P, Farhan H, McEwan DG, Wagner S, Rogov VV, Brady NR, Richter B, Korac J, Waidmann O, Choudhary C, Dotsch V, Bumann D, Dikic I (2011) Phosphorylation of the autophagy receptor optineurin restricts Salmonella growth. *Science* 333 (6039):228–233. <https://doi.org/10.1126/science.1205405>
 18. Kwon YT, Ciechanover A (2017) The ubiquitin code in the ubiquitin-proteasome system and autophagy. *Trends Biochem Sci* 42 (11):873–886. <https://doi.org/10.1016/j.tibs.2017.09.002>
 19. Kuusisto E, Kauppinen T, Alafuzoff I (2008) Use of p62/SQSTM1 antibodies for neuropathological diagnosis. *Neuropathol Appl Neurobiol* 34(2):169–180. <https://doi.org/10.1111/j.1365-2990.2007.00884.x>
 20. Olive M, van Leeuwen FW, Janue A, Moreno D, Torrejon-Escribano B, Ferrer I (2008) Expression of mutant ubiquitin (UBB +1) and p62 in myotilinopathies and desminopathies. *Neuropathol Appl Neurobiol* 34 (1):76–87. <https://doi.org/10.1111/j.1365-2990.2007.00864.x>
 21. Del Grosso A, Angella L, Tonazzini I, Moscardini A, Giordano N, Caleo M, Rocchiccioli S, Cecchini M (2019) Dysregulated autophagy as a new aspect of the molecular pathogenesis of Krabbe disease. *Neurobiol Dis* 129:195–207. <https://doi.org/10.1016/j.nbd.2019.05.011>
 22. Komatsu M, Kurokawa H, Waguri S, Taguchi K, Kobayashi A, Ichimura Y, Sou YS, Ueno I, Sakamoto A, Tong KI, Kim M, Nishito Y, Iemura S, Natsume T, Ueno T, Kominami E, Motohashi H, Tanaka K, Yamamoto M (2010) The selective autophagy substrate p62 activates the stress responsive transcription factor Nrf2 through inactivation of Keap1. *Nat Cell Biol* 12(3):213–223. <https://doi.org/10.1038/ncb2021>

23. Ling J, Kang Y, Zhao R, Xia Q, Lee DF, Chang Z, Li J, Peng B, Fleming JB, Wang H, Liu J, Lemischka IR, Hung MC, Chiao PJ (2012) KrasG12D-induced IKK2/beta/NF-kappaB activation by IL-1alpha and p62 feed-forward loops is required for development of pancreatic ductal adenocarcinoma. *Cancer Cell* 21(1):105–120. <https://doi.org/10.1016/j.ccr.2011.12.006>
24. Marchi S, Corricelli M, Trapani E, Bravi L, Pittaro A, Delle Monache S, Ferroni L, Patergnani S, Missiroli S, Goitre L, Trabalzini L, Rimessi A, Giorgi C, Zavan B, Cassoni P, Dejana E, Retta SF, Pinton P (2015) Defective autophagy is a key feature of cerebral cavernous malformations. *EMBO Mol Med* 7(11):1403–1417. <https://doi.org/10.15252/emmm.201505316>
25. Noda T (2017) Regulation of autophagy through TORC1 and mTORC1. *Biomol Ther* 7(3). <https://doi.org/10.3390/biom7030052>
26. Maes H, Kuchnio A, Peric A, Moens S, Nys K, De Bock K, Quaegebeur A, Schoors S, Georgiadou M, Wouters J, Vinckier S, Vankelecom H, Garmyn M, Vion AC, Radtke F, Boulanger C, Gerhardt H, Dejana E, Dewerchin M, Ghesquiere B, Annaert W, Agostinis P, Carmeliet P (2014) Tumor vessel normalization by chloroquine independent of autophagy. *Cancer Cell* 26(2):190–206. <https://doi.org/10.1016/j.ccr.2014.06.025>
27. Guerrero A, Iglesias C, Raguz S, Florida E, Gil J, Pombo CM, Zalvide J (2015) The cerebral cavernous malformation 3 gene is necessary for senescence induction. *Aging Cell* 14(2):274–283. <https://doi.org/10.1111/acel.12316>
28. Kawasaki J, Aegerter S, Fevurly RD, Mammoto A, Mammoto T, Sahin M, Mably JD, Fishman SJ, Chan J (2014) RASA1 functions in EPHB4 signaling pathway to suppress endothelial mTORC1 activity. *J Clin Invest* 124(6):2774–2784. <https://doi.org/10.1172/JCI67084>
29. Nadal M, Giraudeau B, Tavernier E, Jonville-Bera AP, Lorette G, Maruani A (2016) Efficacy and safety of mammalian target of rapamycin inhibitors in vascular anomalies: a systematic review. *Acta Derm Venereol* 96(4):448–452. <https://doi.org/10.2340/00015555-2300>
30. Marchi S, Retta SF, Pinton P (2016) Cellular processes underlying cerebral cavernous malformations: Autophagy as another point of view. *Autophagy* 12(2):424–425. <https://doi.org/10.1080/15548627.2015.1125073>
31. Otten C, Knox J, Boulday G, Eymery M, Haniszewski M, Neuenschwander M, Radetzki S, Vogt I, Hahn K, De Luca C, Cardoso C, Hamad S, Igual Gil C, Roy P, Albiges-Rizo C, Faurobert E, von Kries JP, Campillos M, Tournier-Lasserre E, Derry WB, Abdelilah-Seyfried S (2018) Systematic pharmacological screens uncover novel pathways involved in cerebral cavernous malformations. *EMBO Mol Med* 10(10). <https://doi.org/10.15252/emmm.201809155>
32. Ridaforolimus (2010) *Drugs in R&D* 10(3):165–178. <https://doi.org/10.2165/11586010-000000000-00000>
33. Schindelin J, Arganda-Carreras I, Frise E, Kaynig V, Longair M, Pietzsch T, Preibisch S, Rueden C, Saalfeld S, Schmid B, Tinevez JY, White DJ, Hartenstein V, Eliceiri K, Tomancak P, Cardona A (2012) Fiji: an open-source platform for biological-image analysis. *Nat Methods* 9(7):676–682. <https://doi.org/10.1038/nmeth.2019>